Mechanical Probe and Modeling Efforts for Evaluation of Plasma Creation and Acceleration in PPT

IEPC-2013-241

Presented at the 33rd International Electric Propulsion Conference,
The George Washington University, Washington, D.C., USA
October 6–10, 2013

Tony Schönherr,* W. Alexander Zach,† and Kimiya Komurasaki‡
The University of Tokyo, Bunkyo, Tokyo, 113-8656, Japan

Sebastian Hörner,§ and Yoshihiro Arakawa¶
The University of Tokyo, Kashiwa, Chiba, 277-8561, Japan

and

Georg Herdrich‖
University of Stuttgart, Stuttgart, Baden-Württemberg, 70569, Germany

Plasma flow behavior during the PPT discharge is highly dependent on time and operation parameters. Combined experimental and numerical work is seen as the key to understand further the processes involved, and to determine future research needs. The application of mechanical probes to measure the Mach number optically is discussed in this study. Values of around 2 were determined for a variation in time, space, and discharge voltage. Numerical efforts were executed concurrently to implement recent experimental results into a combined model. Ablation and ionization processes are implemented, and the final plasma numerically accelerated. In both experimental and numerical work, an inclination of the PPT plasma flow of about 8 deg towards the cathode was observed.

Nomenclature

I	= discharge current
$\dot{m}$	= ablation rate
Ma	= Mach number
q	= heat flux
T	= temperature
t	= time
x	= coordinate along the exhaust direction of the PPT
μ	= upper shock angle
ϑ	= probe angle of the wedge-type probe
σ	= lower shock angle

*Assistant Professor, Department of Aeronautics and Astronautics, schoenherr@al.t.u-tokyo.ac.jp.
†Graduate Student, Department of Aeronautics and Astronautics.
‡Professor, Department of Aeronautics and Astronautics/Department of Advanced Energy.
§Graduate Student, Department of Advanced Energy.
¶Professor Emeritus, Department of Advanced Energy.
‖Associate Professor (Privatodozent), Institute of Space Systems (IRS).

I. Introduction

The discharge of a PPT happens in a timeframe of about 10 µs making it difficult to study either experimentally or numerically due to the strong gradients, non-equilibrium situations, and inhomogeneities. With the availability of experimental equipment capable of recording plasma data in a reasonable temporal and spatial resolution, it became clear that the processes during the discharge are yet far from being understood entirely.[1–3]

Application of mechanical probes to measure inside plasma flows is a very common plasmadiagnostic tool, but has been rarely applied to PPT plasmas yet due to imaging insufficiencies.[4,5] This study, therefore, discusses the feasibility and accuracy of using mechanical probes inside the discharge channel of a PPT, and the capability to derive flow-specific values such as the Mach number from the experiments.

Concurrently, with more computational power and further understanding of the discharge processes, numerical modeling became an essential part of PPT research. With many assumptions remaining, this study uses previous experimental data and observations to build up a numerical model complete with the processes of ablation, ionization, and acceleration of the propellant. Results and issues are discussed.

II. Experimental

In this section, the measurement of the Mach number in the PPT plasma flow by means of wedge-type mechanical probes is discussed.

A. Pulsed Plasma Thruster

The PPT used in this study has a maximum discharge energy of 68 J leading to a total discharge time of less than 20 µs, and the resulting plasma properties were determined as summarized in Table 1. The length of the electrode channel is 75 mm inclined on each side by an angle of 10 deg.[6]

Table 1: Previously determined plasma properties of the PPT plasma flow.

Property	Value	Reference
Electron density	10^{17} cm^{-3}	[1]
Electron temperature	2-3 eV	[1]
Plasma velocity	40-45 km/s	[3]
Knudsen number	10^{-3} - 10^{-2}	[1]
Magnetic flux density	up to 1 T	[2]
Debye length	10^2 - 10^3 nm	-

Due to the relatively small Knudsen number and the continuous ablation process, the PPT plasma flow during the first half-cycle of the discharge is considered a continuum flow. Charged particles are accelerated by the electromagnetic field created by the discharge. The plasma flow direction is, thus, perpendicular to the electric field between the electrodes, and the circular magnetic field around the discharge arc between the electrodes. Although marginal components of the magnetic field exist in the directions parallel to the electric field and parallel to the flow velocity vector, their magnitudes allow for negligence.[2] Therefore, the PPT plasma flow is a magnetized plasma with the magnetic field vector transverse to the flow direction which allows for the application of aerodynamic shock equations rather than MHD shock equations.

B. Vacuum system

The PPT is operated in a ⌀ 0.5 x 1 m steel vacuum chamber equipped with a rotary pump and a turbomolecular pump. Nominal pressure during measurements is about $5 \cdot 10^{-3}$ Pa.

C. Optical system

The high-speed camera used in this study is an Ultra-8 by DRS Hadland LTD Technologies and can record a series of up to eight pictures with a resolution of 520x520 pixels and a minimum exposure time as low as 10 nanoseconds and a minimum hardware delay of 100 ns. The camera is mounted movable in x-direction to change its position along with the probe inside the vacuum chamber. It is equipped with a Nikon 105 mm lens with a manually adjustable aperture. To compensate for the varying light intensity that occurs due to different x-positions and time at which images are recorded, the aperture is adjusted. The aperture size varies between f/2.8 and f/8, and is set manually on the camera lens. A lens with a focal length of 250 mm is installed in the optical path to increase the image size.

D. Mechanical probes

In this study, wedge-type probes of different materials and sizes are used as is shown in Figure 1. As the time of exposure to the plasma is in the order of µs, no cooling of the probes is required. However, as metal might affect the discharge of the PPT, only insulating materials were considered. A measurement of the static pressure was considered too difficult as the probe has small dimensionas, and, therefore, only provides little space for the necessary conduits. Further, the pressure gauge would need to be able to record the rapidly changing pressure of the plasma flow with doubtful accuracy.

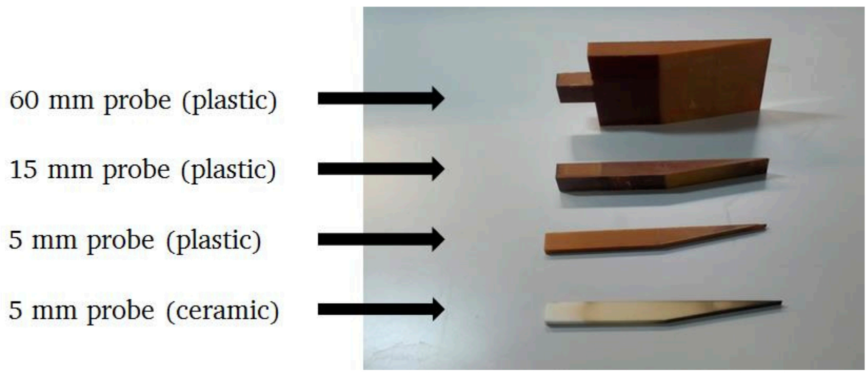

Figure 1: Wedge-type probes used in this study.

In addition, a conical probe was set up to be able to determine the angle of the plasma flow. This was seen necessary as previous measurements indicated that the thrust vector might not be parallel to the center axis of the thruster.[7] Wedge-type probe measurements are only possible when the probe and the plasma flow are aligned.The mount of both probe types is, thus, able to incline all probes by an angle of up to 12 deg.

E. Setup and test parameters

The setup used for the experiments is shown in Figure 2. Next to the vacuum chamber are the power supply units for the main discharge and the ignition. An ignition circuit provides manual triggering of the spark plug. The probe as well as the lens and aperture are mounted on a linear unit. This allows a change of the probes position along the x-axis without opening the vacuum chamber and, thus, reduces the necessary experimental time significantly. The window on the left-hand side of the vacuum chamber is used for the high-speed camera.

Outside the vacuum chamber a photodetector (optical access through right window in Figure 2) is pointed towards the electrodes rear end where the PTFE bar is. Right after ignition the photodetectors signal is amplified, and serves as trigger signal for the pulse generator which in turn triggers the high-speed camera. A computer stores the recorded image series and leaves them for further image processing. Additionally, an oscilloscope is used to record the signals of the photodetector, the high-speed camera, and the discharge voltage signal of the thruster. The voltage is measured using a Yokogawa 700924 differential probe.
In a first series of experiments, the influence of the width and the material of the probe was studied. This was

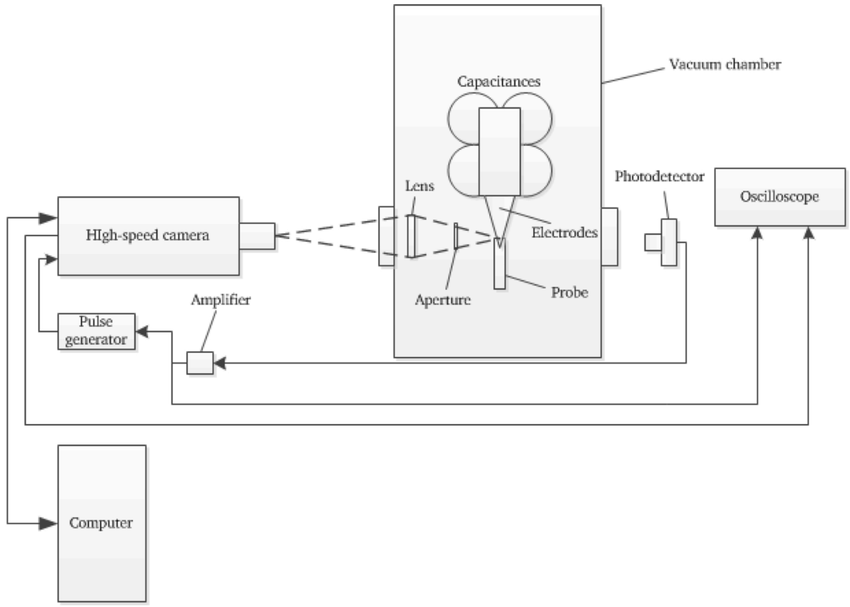

Figure 2: Experimental setup for determination of the Mach number in the plasma flow.

done by comparing the image quality with regard to contrast and brightness as well as the general plasma flow behavior.
Subsequently, experiments were carried out first with the conical probe to determine the inclination of the transient plasma flow. The tip of the probe is situated on the center axis whereas its inclination, the timing of the picture, and the position in x-direction are parameters. Additionally, variations in discharge energy of the PPT are considered. Second, the wedge-type probe considered the best during the preliminary experiments is used to determine the Mach number in the flow using the information of the flow inclination. In this study, the thruster was operated in a breech-fed configuration.
The input energy is varied by adjusting the voltage of the thruster's power supply. Four voltages are used (700, 900, 1100 and 1300 V) to examine the dependence of the Mach number on the energy input. All experiments are carried out using the conical and wedge-type probe which were inclined at different angles to the horizontal (0, 2, 4, 6, 8, 10, 12 degrees).

F. Results and discussion

1. Preliminary tests

High-speed images of the plasma flow over the probe body were successfully taken. Preliminary experiments showed poor intensity for x-positions further than 40 mm and, thus, limit the distribution to values below this threshold. A comparison between the ceramic and the plastic probe showed no significant impact on the resulting image. As the handling and machining of ceramic probes is more delicate and expensive than plastic probes, the latter were chosen for further studies. For the variation in width of the probe, the contrast of the high-speed image was influenced strongly. Using slim probes, the emission from the plasma flow exceeded the shock effect. With plasma glowing in front of the probe body, it was assumed that a proper deflection of the plasma flow was not achieved, and that a three-dimensional flow around the probe body occurs. Using the widest probe with 2-3 times the width of the plasma flow, the visibility of the shock increased significantly, and no plasma emission was observed on the side of the probe body. Thus, the wide probe was chosen for the main experiments.

2. Conical probe

The conical probe was used to determine the angle of attack of the plasma flow. The shock intensity strongly varies over time and the x-position. In images taken at the beginning of the discharge and close to the thrusters propellant the visibility of the shock is still good but it vanishes for positions further away and later in time. If the plasma flow is ideal as shown in Figure 3a, the shock angle of the resulting oblique shocks around the probe match. In the expected real situation of Figure 3b, the probe is adjusted in angle, and the comparison between the upper and lower shock angle yields the inclination of the flow. Note that in Figure 3 the upper electrode is the cathode, the lower electrode is the anode, and the plasma moves from left to right.

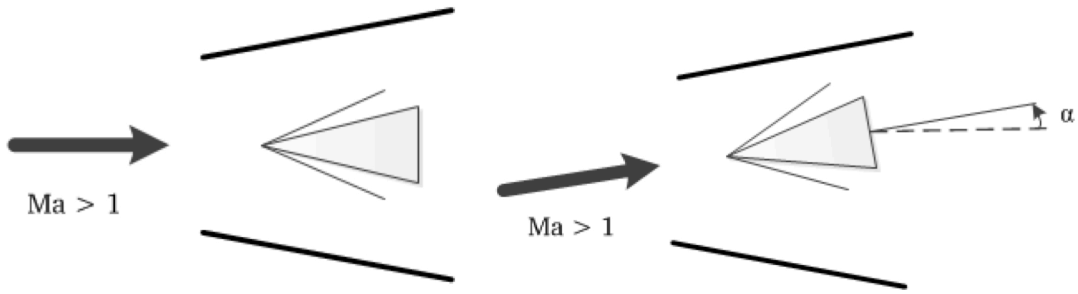

(a) Ideal flow

(b) Real flow

Figure 3: Schematic of plasma flow in the electrode channel over the conical probe.

An exemplary image for the measurements is shown in Figure 4. Here, the probe is not inclined, and a clear difference between the two shock angles can be seen. However, due to the small resolution of the image, a proper detection is made more difficult. This image quality represents the best quality feasible with the system as well as the shock with the optimum contrast, so the error in comparison of the shock angles is significantly higher for the majority of images. However, this error cannot be easily quantified.

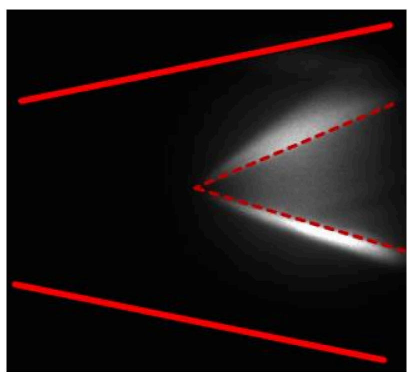

Figure 4: Exemplary image for the experiments with conical probe. Angle of inclination is 0 deg with a full energy discharge, and a x-position of 10 mm.

By variation of the inclination of the probe and the position in x, images were recorded throughout the discharge. By minimizing the difference of the shock angles, the angle of attack (AoA) of the plasma flow was derived and is plotted for the 8 consecutive images of the discharge in Figure 5. It is to be noted that image quality for later images and higher x-values significantly defies proper detection of the shock angle, thus, values should be regarded carefully.

In general, one can see that the angle of attack of the plasma flow reduces as the plasma is further downstream which could be an indication for the stronger influence of the magnetic field rather than the electric field. As the discharge is proceeding, angles seem to vary for individual positions strongly. As this phenomenon cannot be explained, it was decided that measurements with the wedge-type probe would be carried out for all inclinations, and analyzed respectively. The impact on the resulting Mach number is, thus, to be discussed in the following Section.

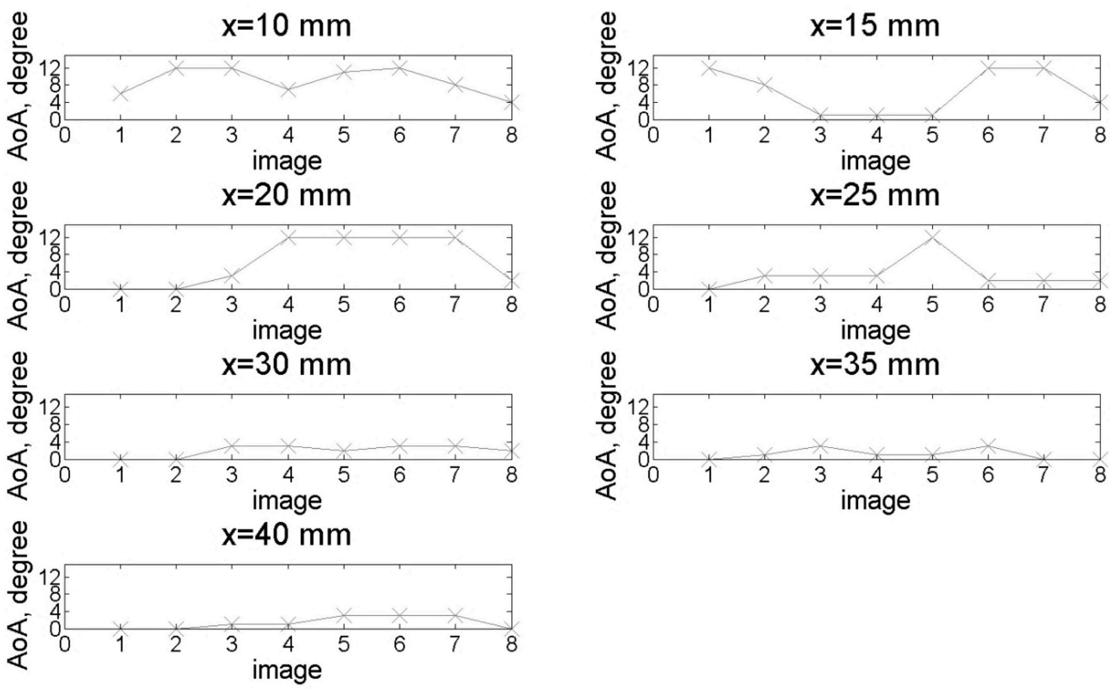

Figure 5: Derived angle of attack of the plasma flow at different positions along the center axis throughout the discharge.

3. Wedge-type probe

Unlike most experiments with the conical probe, the wide wedge-type probe yields a clear shock formation throughout most of the acquired images. Exemplary images throughout the discharge channel are shown in Figure 6. Nevertheless, the further the probe is located the less illuminated is the shock formation resulting in less precise detection of the shock angle.

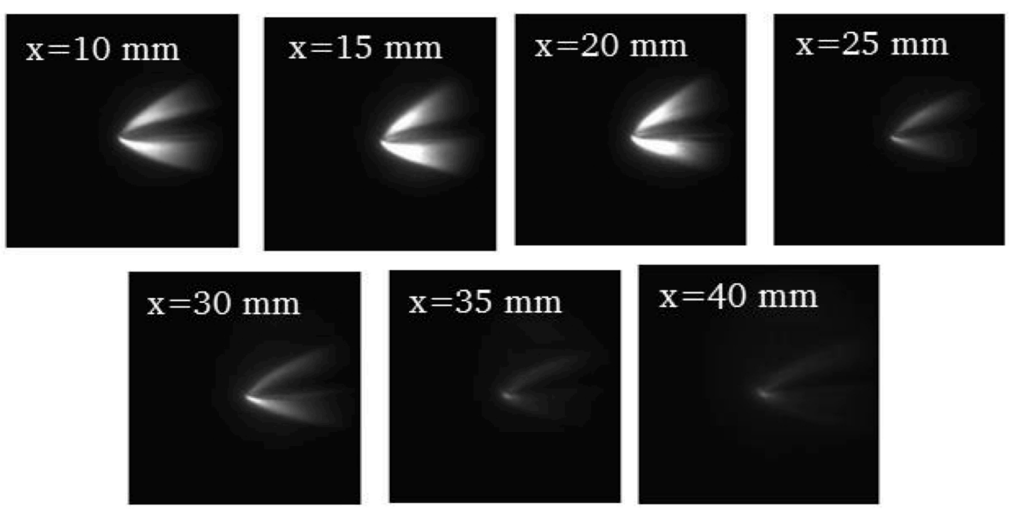

Figure 6: Exemplary images of the shock formation around the wedge-type probe for a variation in x-position. Probe is inclined by 12 deg.

Analysis of the pictures is conducted by measuring the angle on the upper side of the wedge probe μ. Automatic image processing was used, but proved difficult due to the low resolution of the image. With the resulting shock angle, the Mach number Ma is determined by:

$$\sin(\mu) = \frac{1}{\text{Ma}}. \tag{1}$$

Even though the results from the conical probe measurement in Section 2 are not a very reliable source for measuring the angle of attack of the plasma flow over all x-positions and time steps the analysis of the wedge-type probe measurements shows only very minor sensitivity of the resulting Mach number on the angle of inclination. For a variation of probe inclination between 0 and 12 deg for an exemplary x-position, the resulting Mach number is plotted in Figure 7.

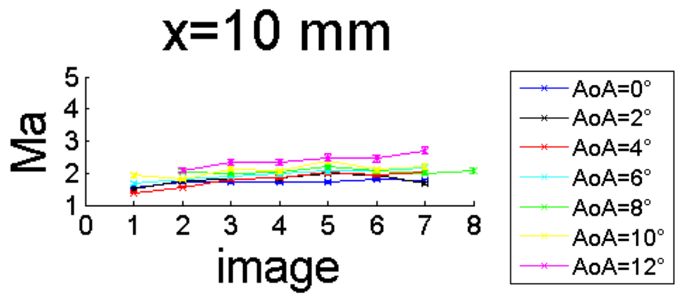

Figure 7: Mach number resulting from wedge probe measurements for a variation in inclination of the probe.

As a result, the Mach number associated with a certain point of measurement is averaged over the various inclinations of the probe, and a standard error derived. The resulting Mach numbers for the investigated parameters are plotted in Figure 8. Values toward the exit of the discharge channel tend to show stronger errors due to the decrease in image quality. Between 10 and 20 mm the Mach numbers are increasing representing the electromagnetic acceleration of the plasma bulk.

As discharge energy is reduced, image quality decreases, but for most investigated voltages the Mach numbers could be derived to be about the same value. This concurs with previous measurements of the plasma velocity.[3] A comparison of the Mach numbers for a position close to the propellant is shown in Figure 9. Discharge voltage and, hence, discharge current and the resulting magnetic field seem to have but a small influence on the Mach number.

From the measurements with the wedge-type probe the lower shock angle σ can be used to determine the adiabatic index γ under the assumption that the latter is constant over the shock. It is then:

$$\tan(\vartheta) = \cot(\sigma)\frac{\text{Ma}^2\sin^2(\sigma) - 1}{1 + \left(\frac{\gamma+1}{2} - \sin^2(\sigma)\right)\text{Ma}^2} \tag{2}$$

Herein, ϑ is the opening angle of the wedge itself. It was found, however, that Equation 2 is very sensitive to slight variations of σ. The uncertainty in the adiabatic index resulting from the measurement errors exceeds ± 1, and is therefore not useful for further discussion here.

III. Numerical

In this section, the plasma flow is treated numerically. As the plasma is created as a result of the ablation and ionization processes during the discharge of the PPT, a modeling of these processes is regarded firstly. The acceleration due to the electromagnetic field is then handled concurrently as the ions are created. The resulting flow information are then used to discuss the general plasma behavior observed in this study and in previous work. Further, resulting performance values are discussed.

A. Ablation phase

Several previous studies discussed the phase of ablation in a PPT discharge. Extensive work at Worcester Polytechnic Institute[8,9] formed the basic model for this study. Modifications were done regarding the material properties and the meshing. Further, the discharge current profile measured for the experimental

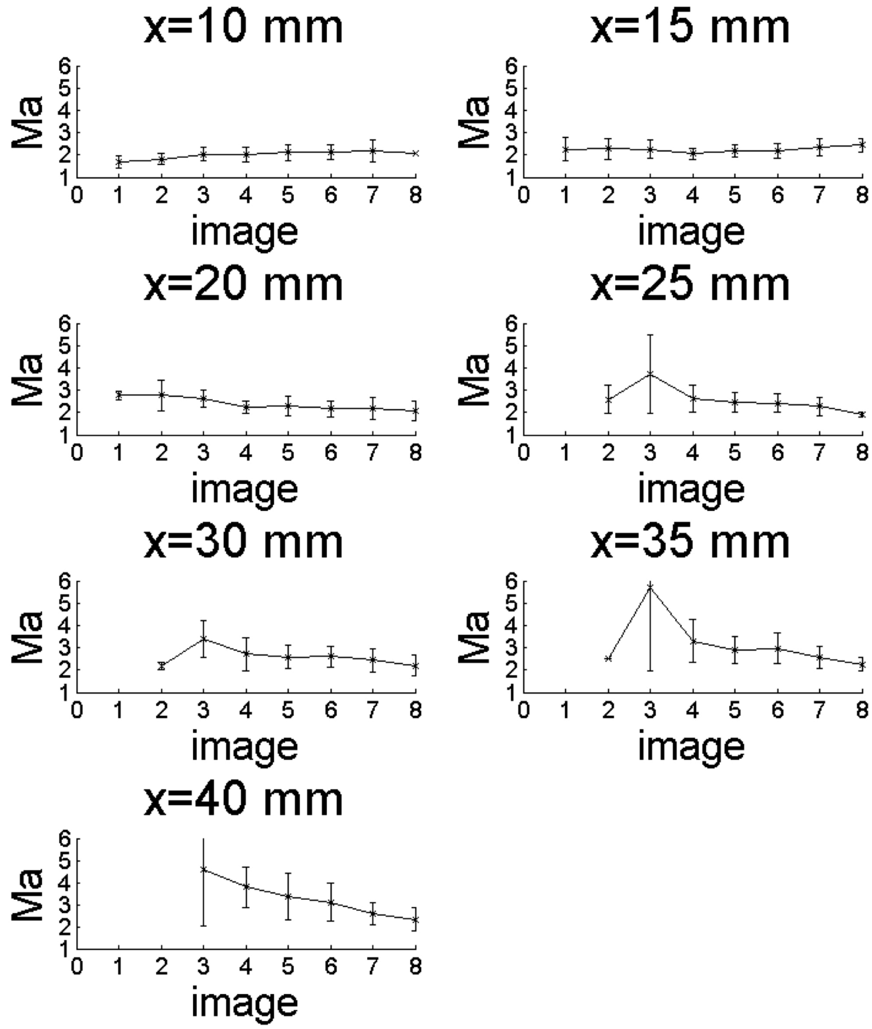

Figure 8: Mach number resulting from wedge probe measurements for a variation in position and time. Data recorded for a PPT operation at maximum energy.

PPT[10] is used to compute a profile of the radiative heat flux proportional to the instantaneous discharge power. From the heat flux, the PTFE temperature and the ablation rate are then computed numerically as a function of time.
This was achieved by using a one-dimensional model with finite differences. It has three key elements. One is the grid spacing, a second the handling of the two phases (initial and amorphous) and the third is the used numerical method to solve the differential equations. On each end of the calculation domain, two ghost cells are added. Ghost cells are not part of the propellant domain. They are used to apply the necessary boundary conditions at the edges of the domain. Mass ablation is considered only in direction of the exposed surface. Solving the thermodynamic differential equations for the used grid, the temperature distribution inside the PTFE block can be derived as is shown in Figure 10.

With the above-mentioned correlation between discharge power and heat flux, experimental values were used to "calibrate" the numerical model, and the resulting values for heat flux and ablation rate as a function of time are plotted in Figure 11.

It can be seen that ablation starts with a delay to the discharge current and for the thruster discussed in this study, is exclusively during the first part of the discharge. Qualitatively the results match other researches,[9,11] but assumptions regarding the discharge arc, the heat flux, and the ablation processes maintain to be a source of possible error.

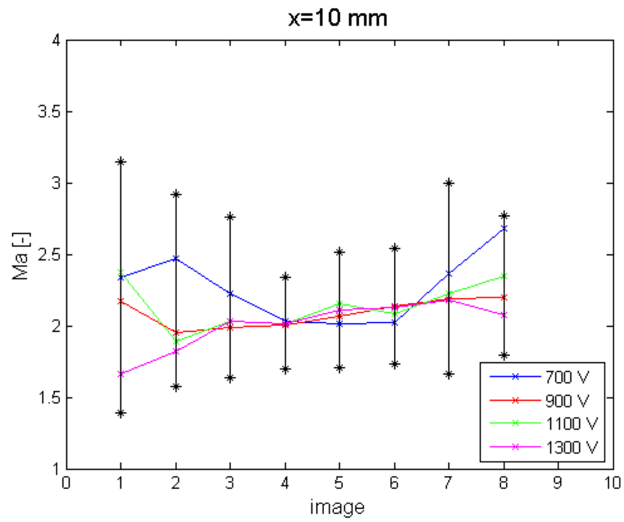

Figure 9: Influence of discharge voltage on the resulting Mach number.

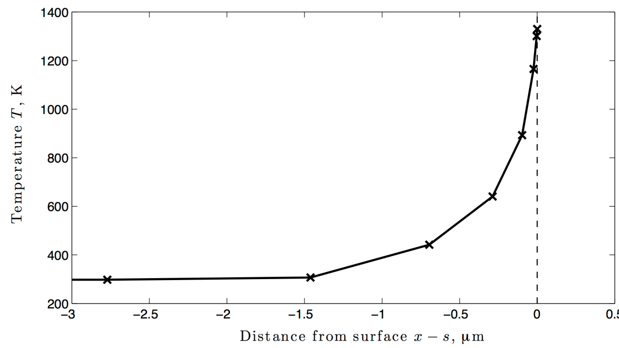

Figure 10: Exemplary one-dimensional temperature profile of the PTFE block.

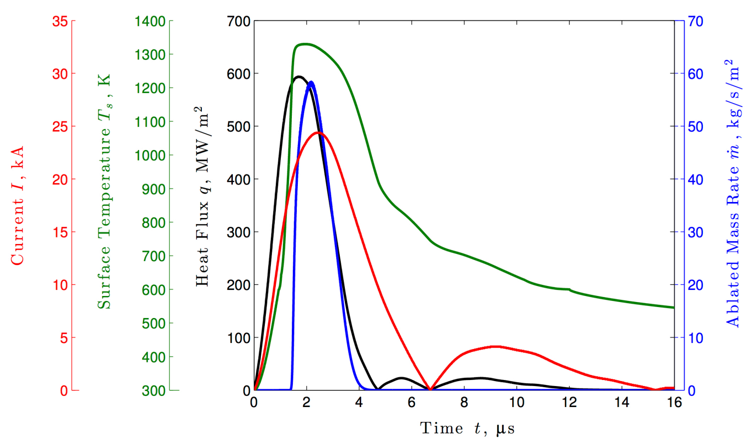

Figure 11: Used heat flux profile and resulting surface temperature and ablation rate as a function of time.

B. Ionization phase

The ablated material that is created by the model of the previous section is heated by the discharge arc towards ionization. To understand the fraction of ionized material for every given point in time, the relation between temperature and ionized particles is necessary. Previous work at the Ohio State University resulted in a model capable to yield this information, and is therefore used as a basis for the model in this study.[12] Computation of the equilibrium equations of the PTFE species yielded similar results as published by OSU, and are shown in Figure 12. Note that slight alterations to the original results are a result of the improved numerical approach, and a higher computation accuracy.

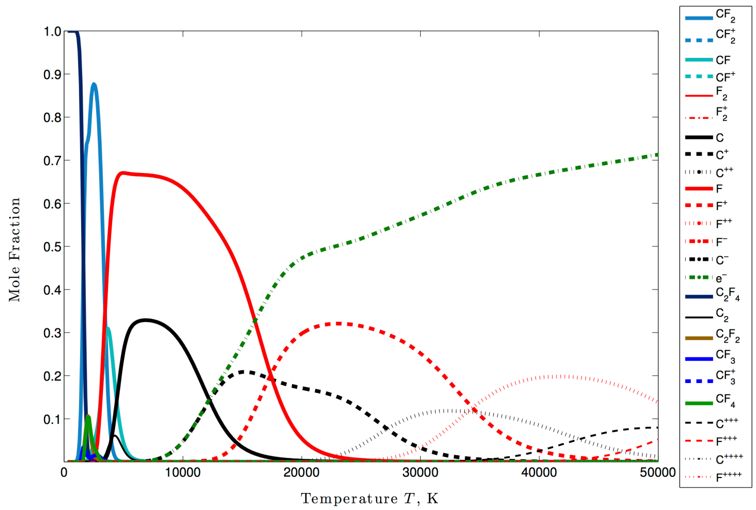

Figure 12: Mole fraction of individual species in a PTFE plasma as a result of the chemical equilibrium considerations (at 1 bar).

With the calibration factors from the ablation model, the temperature of the discharge arc is calculated, and, thus, the composition of the plasma can be determined at each time using the data in Figure 12. The result is an information about how many charged particles are in the forming plasma - the degree of ionization. Figure 13 shows this charged mass ratio as well as the charge per charged mass throughout the discharge. As expected complete ionization is achieved during the initial phase of the PPT discharge whereas partial ionization dominates later discharge phases. As a smaller fraction of mass is involved in these phases, the effect of this less efficient ionization might be small. However, for other PPT configurations it might be essential if many oscillations of the discharge current occur that could yield to a small propellant utilization efficiency.

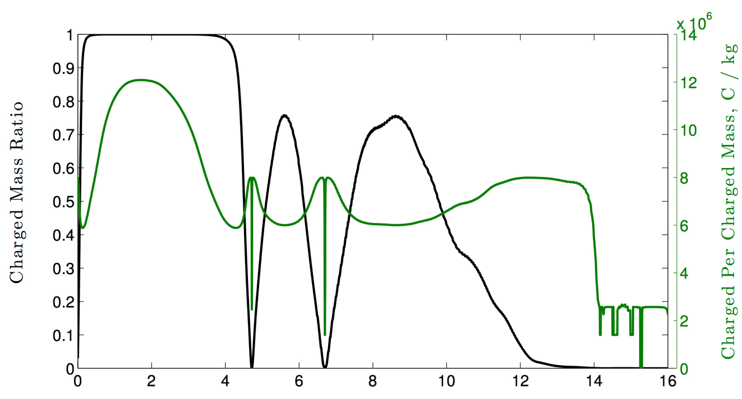

Figure 13: Degree of ionization and charge per mass for the investigated PPT discharge.

The knowledge of charged particles as a function of time is used subsequently as input of the acceleration part of the numerical model.

C. Acceleration phase

Acceleration is a result of the Lorentz force due to the electromagnetic field. With experimental data for discharge voltage and discharge current, the electromagnetic field can be calculated as a function of time and applied to the charged particles. As the computation space is limited by the electrodes and the propellant surface, the position of ion production is essential for the subsequent movement. Particles close to the cathode might hit the electrode before they reach the end of the electrode. Due to limitations of computational power, a distribution of ion production is simulated by three starting points across the surface (center, cathode side, anode side). The totally ablated mass is distributed equally among those, and their movement then traced. It was found that this phase is sensitive to the position of the discharge arc as its resulting magnetic field shows a strong impact. Unfortunately, the behavior of the discharge arc is yet unknown, and, hence, the resulting exhaust velocities exceed slightly the measured values. The inclination of the plasma flow was, however, deduced to be around 8 deg towards the cathode which would agree quite well with the experimental results in Figure 5. Further investigation of the discharge arc could yield to a more precise determination of the performance behavior.

IV. Conclusion

Measurement of the Mach number during the PPT discharge and inside the discharge channel by means of a wedge-type probe and a high-speed imaging setup yielded Mach numbers around 2 that were hardly affected by a variation of discharge voltage. This might require further study as the scaling of the electromagnetic fields with the voltage might suggest otherwise. Resolution of the imaging system is not high enough to deduce further plasma parameters like the adiabatic index within reasonable errors. Accelerative behavior was observed for measurement points closer to the propellant surface verifying theoretical assessment. An inclination of the plasma flow towards the cathode was observed to be around 5-10 deg.

A similar inclination is the numerical result of a three-component model computing ablation, ionization, and acceleration of the propellant. That the inclination of the plasma flow concurs with the inclination of the electrodes can be an explanation for the performance optimum.[6] Assumptions concerning the nature and movement of the discharge arc during the discharge remain to have a strong impact on the numerical results, and further studies in this field are recommended.

Acknowledgments

The authors want to thank Mr. Kohei Shimamura for experimental help.

References

[1]Schönherr, T., Nees, F., Arakawa, Y., Komurasaki, K., and Herdrich, G., "Characteristics of plasma properties in an ablative pulsed plasma thruster," *Physics of Plasmas*, Vol. 20, No. 3, March 2013, pp. 033503–1–8.

[2]Lau, M., Manna, S., Herdrich, G., Schönherr, T., and Komurasaki, K., "Experimental Investigation of the Current Density in the Discharge Plasma of ADD SIMP-LEX," 48th AIAA/ASME/SAE/ASEE Joint Propulsion Conference, July-Aug. 2012, AIAA-2012-4275.

[3]Schönherr, T., Komurasaki, K., and Herdrich, G., "Propellant utilization efficiency in a pulsed plasma thruster," *Journal of Propulsion and Power*, 2013, (in print).

[4]Di Capua, M. S., *Energy Deposition in Parallel-Plate Plasma Accelerators*, Ph.d. thesis, Princeton University, Princeton, NJ, USA, Dec. 1971.

[5]Antropov, N. N., Diakonov, G. A., Orlov, M. M., Popov, G. A., Semenikhin, S. A., Tyutin, V. K., and Yakovlev, V. N., "Study of Physical Processes and Performance of Ablative Pulsed Plasma Thrusters," Space Propulsion, May 2010.

[6]Schönherr, T., Nawaz, A., Herdrich, G., Röser, H.-P., and Auweter-Kurtz, M., "Influence of Electrode Shape on Performance of Pulsed Magnetoplasmadynamic Thruster SIMP-LEX," *Journal of Propulsion and Power*, Vol. 25, No. 2, March-April 2009, pp. 380–386.

[7]Scharlemann, C. A. and York, T. M., "Mass Flux Measurements in the Plume of a Pulsed Plasma Thruster," 42nd AIAA/ASME/SAE/ASEE Joint Propulsion Conference, July 2006, AIAA-2006-4856.

[8]Stechmann, D. P., *Numerical Analysis of Transient Teflon Ablation in Pulsed Plasma Thrusters*, Master thesis, Worcester Polytechnic Institute, Worcester, MA, USA, July 2007.

[9]Gatsonis, N. A., Juric, D., and Stechmann, D. P., "Numerical Analysis of Teflon Ablation in Pulsed Plasma Thrusters," 43rd AIAA/ASME/SAE/ASEE Joint Propulsion Conference, July 2007, AIAA-2007-5227.

[10]Schönherr, T., Komurasaki, K., Kawashima, R., Arakawa, Y., and Herdrich, G., "Effect of Capacitance on Discharge Behavior of Pulsed Plasma Thruster," *Journal of IAPS*, Vol. 18, No. 1, June 2010, pp. 23–28.

[11]Kazeev, M. N. and Kozlov, V. F., "Ablation-Fed Discharge Characteristics," 31st International Electric Propulsion Conference, Sept. 2009, IEPC-2009-249.

[12]Schmahl, C. S., *Thermochemical and Transport Processes in Pulsed Plasma Microthrusters: A Two-Temperature Analysis*, Ph.d. thesis, Ohio State University, Columbus, OH, USA, 2002.